Share Your Innovations through JACS Directory

Journal of Nanoscience and Technology

Visit Journal at http://www.jacsdirectory.com/jnst

ISSN: 2455-0191

Synthesis and Structural Investigations of ZnO–SnO_2 Nanocomposite by Sol–Gel Method

V. Muthupriyal[1], D. Muthu Raj[1], E. Kumar[2,*]

[1]*Department of Physics, The M.D.T. Hindu College, Tirunelveli – 627 010, Tamil Nadu, India.*
[2]*Department of Physics, School of Science, Tamil Nadu Open University, Chennai – 600 015, Tamil Nadu, India.*

ARTICLE DETAILS

Article history:
Received 11 April 2017
Accepted 23 April 2017
Available online 25 April 2017

Keywords:
Nanocomposite
Metal-Oxide Nanoparticles
XRD

ABSTRACT

In this work the preparation of ZnO-SnO_2 nanocomposites from ZnO and SnO_2 nanoparticles produced by Sol – Gel method. Zinc acetate dihydrate ($Zn(CH_3COO)_2 \times 2H_2O$) and tin(II) chloride dehydrates ($SnCl_2.2H_2O$) have been used as precursors. The structural investigation of ZnO - SnO_2 reveal that the ZnO nanoparticle is hexagonal in structure and SnO_2 nanoparticle is tetragonal. Nanocompsites in two different molarities synthesized by Sol – Gel method. The Miller indices and the crystalline size ZnO-SnO_2 nanocomposites show that the particle size in two different molarities is 62.55 nm and 59.25 nm were determined by powder XRD technique. The spectroscopic functional groups of ZnO-SnO_2 nanocomposite were carried out by FT-IR. The absorbance band and the band gap energy of ZnO-SnO_2 nanocomposite were calculated from the UV – visible spectrum.

1. Introduction

ZnO, as semiconducting II-VI metal oxide with wide band gap 3.37 eV. ZnO possess potential material for many devices applications such as gas sensor, solar cells, optoelectronic devices and LED. SnO_2 is n-type material with the band gap 3.5-3.6 eV. SnO_2 has been applied for various applications such as solar cells, lithium ion batteries and gas sensor. SnO_2 have received attention from many researcher studied on gas sensor application for having high sensitivity and relatively low operating temperature. ZnO and SnO_2 have unique properties due to their chemical and physical properties. Mixing ZnO and SnO_2 could form various kind of composite material such as ZnO/SnO_2, $ZnSnO_3$, $Zn2SnO_4$, Zn-doped SnO_2 and Sn-doped ZnO. Different type of ZnO/SnO_2 structured have been prepared such as nanofibers, nanorod, nanoflowers [1-5].

Different method such as thermal decomposition, chemical vapor deposition, thermolysis, spray pyrolysis, condensation, hydrothermal and also available in literature to synthesize ZnO-SnO_2 nanocomposites. In this experiment, ZnO -SnO_2 nanocomposites were synthesized using sol-gel method in two different molarities as this method has several advantages such as short reaction time and easily synthesized. The aim of this project was to study the structural investigation ZnO–SnO_2 nanocomposites in two different molarities [5-10].

2. Experimental Methods

2.1 Materials

All the chemical were used as analytical grade without any further purification. Zinc acetate dehydrate ($Zn(CH_3COO)_2.2H_2O$), tin chloride dehydrate($SnCl_4.2H_2O$), methanol and ammonia were used to prepare the ZnO-SnO_2 nanocomposites for this study.

2.2 Synthesis of ZnO - SnO_2 Nanocomposites

Zinc acetate dehydrate and tin chloride dehydrate were used as starting materials. Methanol and ammonium hydroxide solution were used as solvent and additive, respectively. All chemicals were analytical grade (AR) and used without further purification. The synthesis of the ZnO – SnO_2 mixed photo catalyst started by slowly adding a 0.01 M methanol of $Zn(CH_3COO)_2.2H_2O$, previously prepared 0.01 M methanol solution of $SnCl_4.2H_2O$ prepared in the same conditions. Typically, 0.812 g of $Zn(CH_3COO)_2.2H_2O$ were dissolved in 37 mL of methanol and the amount of $SnCl_4.2H_2O$ solution was opportunely dissolved in order to obtain powders with the molar ratio ZnO-SnO_2 equal to 0.01/0.01 and 0.01/0.025 respectively. The obtained solutions were continuously stirred for 2h, keeping the 80 °C. Then, the NH_4OH solution was added dropwise until pH reached the value of pH 8. The solutions became gels which were dried produce xerogels. Finally, the pure oxides were synthesized in the same way by using only the corresponding precursor.

2.3 Instrumentation

The prepared (ZnO-SnO_2) nanocomposites were characterized by powder XRD using an X-ray diffractometer (Model Bruker D-8). FTIR spectra of prepared (ZnO-SnO_2) nanocomposites were characterized by Jasco 4100 spectrophotometer, and UV spectra of the prepared (ZnO-SnO_2) nanocomposites were characterized by UV-1700 series spectrophotometer in the absorption mode.

3. Results and Discussion

3.1 Structural Characterization

3.1.1 XRD Studies

The prepared ZnO-SnO_2 nanocomposites were characterized study by different characterization techniques. The structure and phase purity of the powders was examined by powder X-ray diffraction (XRD) technique using an X-ray diffractometer (Model Brucker D-8with Nickel filtered Cu K_α (λ = 0.15404 nm) radiation.

The crystal phase composition of ZnO–SnO_2 nanocomposites was determined by the XRD analysis; the diffractograms were recorded in range of 10-80°. Figs. 1 and 2 displays XRD patterns of synthesized ZnO–SnO_2 nanocomposites. The existence of strong and sharp diffraction peaks located at 26.2°, 38.2°, 44.52°, and 78.71° corresponding to (110), (200), (204) and (321) planes, respectively. All the peaks can be readily indexed to crystalline size of SnO_2 nanocomposites (standard data of JCPDS file number of 88-0287) with tetragonal phase (a=b= 0.4737 nm and c= 0.3186 nm) and the existence of strong and sharp diffracted peaks located at 32.69°, 46.44°, 65.02° and 73.62° corresponding to (100), (004), (200) and (102) planes, respectively. All the peaks can be readily indexed to crystalline size of ZnO nanocomposites (standard data of JCPDS file number of 89-7102) with hexagonal phase (a=b= 0.3249 nm and c= 0.5206 nm) from some of previous works [11, 12].

*Corresponding Author
Email Address: kumarnano@gmail.com (E. Kumar)

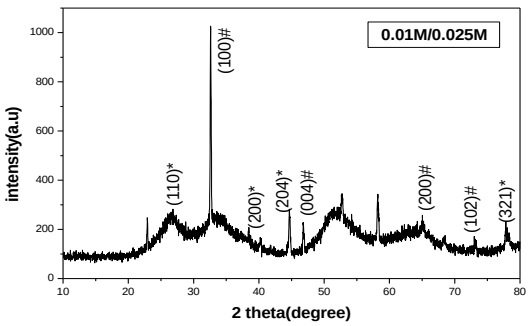

Fig. 1 XRD Pattern of ZnO - SnO_2 nanocomposites (0.01 M/ 0.025 M)

Table 1 XRD data of the ZnO-SnO_2 (0.01 M/0.025 M) nononanocomposites

2θ	Cos θ (Radian)	FWHM β (Radian)	βCosθ x10^{-3}	Size (nm)	D Spacing (Å)
26.90	0.01697	0.1004	1.703	81.34	3.8820
32.59	0.01675	0.1338	2.241	61.83	2.7475
44.70	0.01614	0.2007	3.239	42.78	2.0271
46.82	0.01601	0.1338	2.143	64.67	1.9401

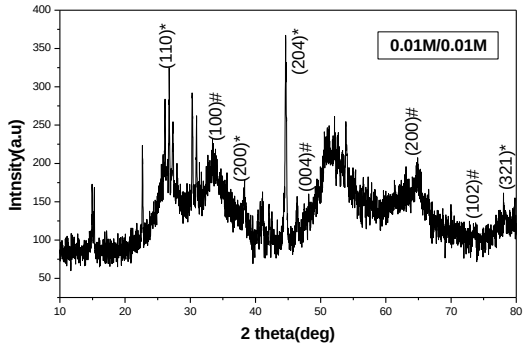

Fig. 2 XRD Pattern of ZnO - SnO_2 nanocomposites (0.01 M/ 0.01 M)

Table 2 XRD data of the ZnO-SnO2 (0.01 M/0.01 M) nanocomposites

2θ	Cos θ	FWHM β (Radian)	β Cosθ x10^{-3}	Size (nm)	D Spacing (Å)
26.76	0.9729	0.1004	1.70	81.31	3.4110
44.61	0.9252	0.1338	2.16	64.16	2.0311
46.39	0.9192	0.2676	4.29	32.29	1.9571

3.2 Particle Size Calculation

From this study, considering the peak at degrees, average particle size has been estimated by using Debye-Scherer formula. Inter-planar spacing between atoms (d-spacing) is calculated using Bragg's law and enumerated in Tables 1 and 2.

$$D = 0.9\lambda/\beta \cos\theta \quad (1)$$

$$2d \sin\theta = n\lambda \quad (2)$$

where, λ is wavelength of X-Ray (0.1540 nm), β is FWHM (full width at half maximum), θ is diffraction angle, d is d-spacing and D is particle diameter size and n is the order of diffraction.

The size of the ZnO - SnO_2 nononanocomposites 62.655 nm in 0.01 M / 0.025 M and size of the ZnO-SnO_2 nononanocomposites 59.25 nm in 0.01 M/0.01 M.

3.3 FT-IR Spectral Analysis

The presence of fuctional groups of the as-prepared ZnO-SnO_2 nanocomposites was synthesized by the sol – gel method is analyzed using FT-IR spectroscopy. The Infrared spectra of the samples are recorded in the range 400-4000 cm^{-1} on a JASCO 4100 Fourier Transform Infrared (FT-IR) spectrometer. The powder samples are finely dispersed in KBr using an agate mortar and ground well. The finely dispersed materials are then pressed in the form of circular discs of nearly 10 mm diameter and 0.5 mm thickness at a pressure of 250 MPa. These pellets are then dried with IR light before the FT-IR spectrum has been recorded.

The FT-IR spectrum of as-prepared ZnO-SnO_2 nanocomposites is shown in the Figs. 3 and 4 and the corresponding functional groups are listed in the Tables 3 and 4. In FTIR spectrum the peaks observed at 3435 cm^{-1}, 3337 cm^{-1} and 1509 cm^{-1}, 1572 cm^{-1} are attributed to O – H [13] stretching vibration and H – O – H bending vibration respectively due to the existence of small amount of water in the ZnO-SnO_2 nanocomposites. A peak observed 1406 cm^{-1} and 1397 cm^{-1} due to the carbonyl group [14] present in the ZnO-SnO_2 nanocomposites. In general, the peak observed between 400 cm^{-1} - 600 cm^{-1} is ascribed to metal – oxygen (M - O) i.e. Zn - O stretching vibration. The absorption band located around 562 cm^{-1} is because of the stretching vibration of ZnO [15]. In the spectrum the absorption peak at 641 m^{-1} is to do with the Sn-O [16] stretching vibration. Due to the change in molarities of O-Sn – O the peak value are merged together. Absorbance band around at 641 cm^{-1} could be attributed to O-Sn - O, Sn- O or O-Sn-O lattice [17]. The peak appeared around 1116 cm^{-1} 1244 cm^{-1} is due to δ (SnOH) vibration [18].

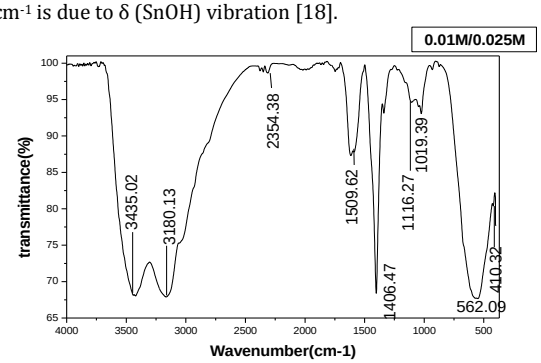

Fig. 3 FTIR Spectrum of the ZnO-SnO_2 nanocomposites

Table 3 Functional group of the ZnO-SnO_2 nanoparticles

Wave numbers (cm^{-1})	Assignments
3435.02	H_2O Anti symmetric stretching vibration
1406.47	H_2O symmetric bending vibration
1116	δ (Sn-OH) Vibration
410.32	Zn – O stretching vibration and
562.09	Sn – O stretching vibration merge with the Zn –O stretching vibration

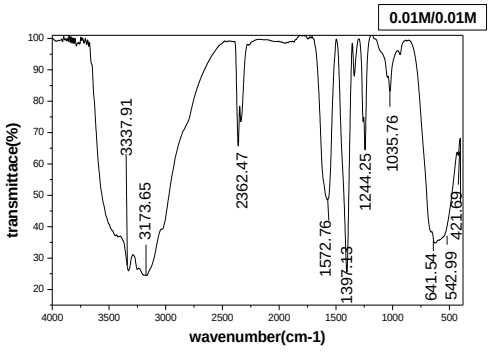

Fig. 4 FTIR Spectrum of the ZnO-SnO_2 nanocomposites

Table 4 Functional group of the ZnO-SnO2 nanocomposites

Wave numbers (cm^{-1})	Assignments
3337.91	H_2O Anti symmetric stretching vibration
1396.13	H_2O symmetric bending vibration
1244	δ (Sn-OH) Vibration
542.99 and 421.69	Zn – O stretching vibration
641.54	O- Sn - O stretching vibration

3.4 UV Analysis

Optical absorption studies were carried out by ultrasonically dispersing the samples in spectroscopic grade DMSO (dimethyl sulfoxide). The room temperature ultraviolet-visible spectra of ZnO-SnO_2 nanocomposites samples were recorded using UV-1700 series spectrophotometer in the absorption mode. The UV-absorption edge provides a reliable estimate of the band gap of any system. The optical absorption spectra of the ZnO-SnO_2 nanocomposites are presented in Figs. 5 and 6. The absorption peak were observed in 231.48 nm and 230.55 nm and The band gap energy was calculated by plotting the optical energy hν against $(\alpha h\nu)^2$ for ZnO – SnO_2 nanocomposites and the plot is shown in Fig. 7. The obtained bandgap value is 2.45 eV. It is due to the merging of band gap value of ZnO –SnO_2 [19, 20].

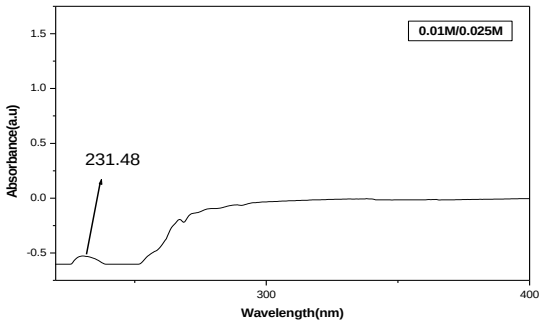

Fig. 5 UV-Vis absorption spectrum of ZnO-SnO_2 nanocomposites

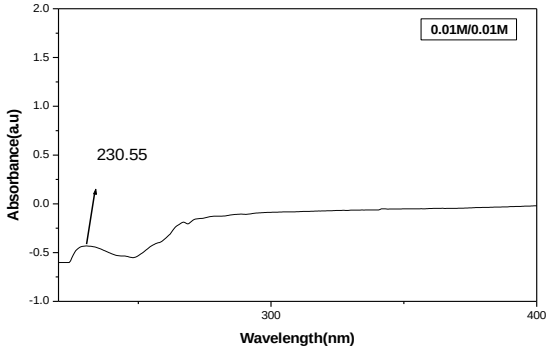

Fig. 6 UV-Vis absorption spectrum of ZnO-SnO_2 nanocomposites

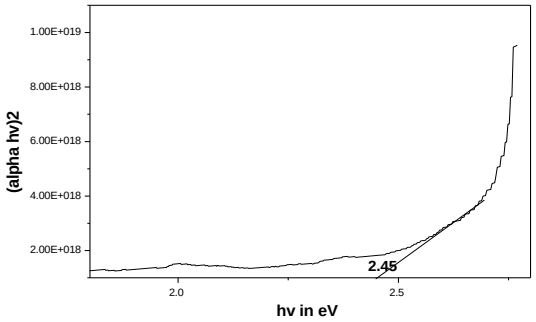

Fig. 7 the band gap energy of the ZnO-SnO_2 nanocomposites

4. Conclusion

In summary, ZnO-SnO_2 nanocomposites have been successfully synthesized by sol – gel method. The structural properties reveal that the ZnO nanoparticle is hexagonal in structure and SnO_2 nanoparticle is tetragonal. The Miller Indices and the crystalline size ZnO-SnO_2 nanocomposites show that the particle size in two different molarities is 62.55 nm and 59.25 nm were determined by powder XRD technique. The phase purity and functional groups of the samples were analyzed by FT-IR studies. The optical absorption spectra of the ZnO - SnO_2 nanocomposites the absorption peaks were observed .The Band gap energy of the ZnO-SnO_2 nanocomposites is 2.45 eV. The UV Visible absorption spectra of ZnO – SnO_2 nanocomposites exhibited blue shift.

References

[1] G. Singh, A. Choudhary, D. Haranath, A.G. Joshi, N. Singh, et al, ZnO decorated luminescent graphene as a potential gas sensor at room temperature, Carbon 50 (2012) 385-394.

[2] C.S. Chou, F.C. Chou, Y.G .Ding, P.Wu, The effect of ZnO-coating on the performance of a dye-sensitized solar cell, Solar Ener. Adv. Mat. Res. 88(6) (2012) 1435-1442.

[3] I.Y.Y. Bu, Y.M. Yeh, Effects of sulfidation on the optoelectronic properties of hydrothermally synthesized ZnO nanowires, Ceramics Int. - Int. J. Photoener. 2012 (2012) 268173.

[4] M. Carotta, A. Cervi, A. Fioravanti, S. Gherardi, A. Giberti, et al, A novel ozone detection at room temperature through UV-LED-assisted ZnO thick film sensors, Thin Solid Films 520 (2011) 939-946.

[5] Z. Chen, Y. Tian, S. Li, H. Zheng, W. Zhang, Electrodeposition of arborous structure nanocrystalline SnO_2 and application in flexible dye-sensitized solar cells, J. Alloys Compds. 2011 (2011) 960487.

[6] X. Wang, X. Zhou, K. Yao, J. Zhang, Z. Liu, A SnO_2 graphene composite as a high stability electrode for lithium ion batteries, Carbon 49 (2011) 133-139.

[7] X. Ma, Towards enhanced SnO_2 gas sensor: Mini-review, J. Nanoengg. Nanomanuf. 2(1-4) (2012) 143-149.

[8] A. Chen, X. Huang, Z. Tong, S. Bai, R. Luo, et al, Preparation, characterization and gas-sensing properties of SnO_2–In_2O_3 nanocomposite oxides, Sens. Actuat. B Chem. 115 (2006) 316-321.

[9] J. Elias, J. Michler, L. Philippe, M.Y. Lin, C. Couteau, et al, ZnO nanowires, nanotubes, and complex hierarchical structures obtained by electrochemical deposition, J. Electronic Mat. 40 (2011) 728-732.

[10] L .Chen, C. Li, W.L. Yin, J. Liu, L. Hei, et al, Effect of deposition temperature and quality of free-standing diamond substrates on the properties of RF sputtering ZnO films, Diamond Relat. Mat. 20 (2011) 527-531.

[11] M. Maleki, S. Rozati, Structural, electrical and optical properties of transparent conducting SnO_2 films: effect of the oxygen flow rate, Physica Scripta 86 (2012) 015801.

[12] C.G. Kang, J.W. Kang, S.K. Lee, S.Y. Lee, C.H. Cho, et al, Characteristics of CVD graphene nanoribbon formed by a ZnO nanowire hardmask, Nanotechnol. 22 (2011) 295201.

[13] A.J. Reddy, M.K. Kokila, H. Nagabhushana, R.P.S. Chankradhar, C. Shivakumara, et al, Structural, optical and EPR studies on ZnO: Cu nanopowders prepared via low temperature solution combustion synthesis, J. Alloys Compds. 509(17) (2011) 5349-5355.

[14] Y. Zhang, L. Wu, H. Li, J. Xu, L. Han, B. Wang, Z. Tuo, E. Xie, Influence of Fe doping on the optical property of ZnO films, J. Alloys Compds. 473 (2007) 319-322.

[15] R. Elilarasi, G. Chandrasekaran, J. Amer, Structural, optical and electron paramagnetic resonance studies on Cu-doped ZnO nanoparticles synthesized using a novel auto-combustion method, Front Master Sci. 7 (2007) 196-201.

[16] S. Mihaiu, I. Atkinson, O. Mocioiu, A. Toader, E. Tenea, Spectroscopic investigations of the formation of the Zn-Sn-O nanostructured films, Mater. Acad. Română Rev. Roumaine de Chim. 57(4-5) (2012) 477-490.

[17] Abbasi, S. Zebarjad, S.M. Baghban, A. Youssefi, Synthesis of TiO2 and decorated multiwalled carbon nanotubes with various content of rutile titania, Syn. React. Inorg. Met. Org. Nano Met. Chem. 45 (2015) 1539-1548.

[18] X.S. Fang, C.H. Ye, L.D. Zhang, T. Xie, Twinning-mediated growth of al_2o_3 nanobelts and their enhanced dielectric responses, Adv. Mater. 17 (2005) 1661-1665.

[19] Y.N. Xia, P.D.Yang, Y.G. Sun, Y.Y. Wu, B. Mayers, et al, One-dimensional nanostructures: synthesis, characterization, and Applications, Adv. Mater. 15 (2003) 353-389.

[20] S.H. Yu, B. Liu, M.S. Mo, J.H. Huang, X.M. Liu, et al, General synthesis of single-crystal tungstate nanorods/nanowires: a facile, low temperature solution approach, Adv. Funct. Mater. 13 (2003) 639-647.